PROCEEDINGS OF THE NATO ADVANCED RESEARCH WORKSHOP ON SUPERDENSE QCD MATTER AND COMPACT STARS

Yerevan, Armenia, 27.09. - 4.10. 2003

Edited by

DAVID BLASCHKE
Rostock University and JINR Dubna

DAVID SEDRAKIAN
Yerevan State University

Kluwer Academic Publishers
Boston/Dordrecht/London

SUPERDENSE STARS WITH A QUARK CORE

G. B. Alaverdyan
Yerevan State University, Alex Manookian 1, Yerevan 375025 , Armenia
galaverdyan@ysu.am

A. R. Harutyunyan
Yerevan State University, Alex Manookian 1, Yerevan 375025 , Armenia
anharutr@ysu.am

Yu. L. Vartanyan
Yerevan State University, Alex Manookian 1, Yerevan 375025 , Armenia
yuvartanyan@ysu.am

Abstract Series of neutron star models with strange quark cores are constructed on the basis of an extensive set of calculated realistic equations of state of superdense matter with quark-hadron phase transition. For some models a new local maximum on the stable branch of the star mass -central pressure diagram is revealed. This maximum arises along with the appearance of a sharp fracture on the core, which is characteristic for models of layered stars with $\lambda > 3/2$ (λ is the relativistic parameter of the density jump) and corresponds to the beginning of formation of a new phase. Such a new local maximum is discovered in the mass range of about $M \sim 0.08 M_\odot$ in some models, as well as at $M \sim 0.82 M_\odot$ in others. Stable equilibrium layered neutron stars, located in these ranges, are characterized also by unusually large values of the stellar radius (from $R \sim 1300$ km to $R \sim 2700$ km for different equations of state). For such equations of state accretion onto a neutron star will lead to two successive jumplike transitions to a quark-core neutron star; as a result, there will be two successive energy releases.

Keywords: Neutron stars, strange quark core, quark phase transition, new branch of stability, accretion

1. Introduction

At superhigh densities a phase transition is possible from the state in which quarks are confined within the baryons, to a continuum quark plasma [1]. At

present an exact theoretical description of matter both in baryon and quark-gluon density ranges is not possible. This makes it very important to study the dependence of parameters of superdense stellar objects on the variants of equation of state (EoS). In many studies models of strange stars were comprehensively analyzed. However, much fewer studies are devoted to configurations with a density jump [2, 4–9]. The most complete calculations of models with a mixed phase are in Refs. [11, 13, 12, 10, 14], which contain various quark configurations in the form of droplet, rodlike, and platelike structures; these models assume continuous energy and density variations in the quark-phase formation region [15]. The results of these authors show that the formation of the mixed phase of quark and nuclear matter may be energetically more or less favorable than an ordinary first-order nucleon-to-quark phase transition, depending on the local surface and Coulomb energies associated with the formation of mixed-phase quark and nuclear structures [11, 13]. Because of uncertainty in the interface tension of strange quark matter, we presently cannot unambiguously establish which of the above alternatives is actually realized [10, 16]. Below, we consider the case that assumes an interface tension that leads to a first-order phase transition with the possible coexistence of the two phases. In the present work, we study the functional dependence of integral parameters and structural characteristics of layered neutron stars with a strange quark core on the form of EoS of superdense matter with first order phase transition to strange quark state. Series of models of neutron stars with strange quark cores are constructed, based on an extensive set of calculated realistic equations of state. The parameters of some characteristic configurations of the calculated series are also presented, and their thorough investigation is carried out. For some models of EoS the possibility of a new additional range of stability for neutron stars with strange quark cores is revealed.

2. Equations of state

In the present work we carry out a thorough study of layered configurations with a density jump, containing strange quark core. By combination of the three EoS of neutron matter with different variants of strange quark-electron plasma calculated within the framework of MIT quark "bag" model [17], we constructed an extensive set of realistic EoS with a quark phase transition. Table 1 gives the variants of the EoS used for the quark component, as well as the values of the energy per baryon ε_{min} and the baryon density n_{min} at the minimum point. If the energy per baryon ε in strange quark phase has a positive minimum ε_{min}, a thermodynamic equilibrium between the quark matter and the baryon component may take place that is realized in neutron stars with a quark core. At subnuclear and supranuclear densities, we used relativistic EoS for neutron matter that were calculated and tabulated by Weber, Glen-

	m_s MeV	B MeV/fm^3	α_c	$\varepsilon_{\min}$ MeV	$n_{\min}$ fm^{-3}
a	175	55	0.5	10.44	0.258
b	200	55	0.5	20.71	0.263
c	175	55	0.6	28.61	0.258
d	175	60	0.5	28.97	0.276
e	200	55	0.6	38.24	0.259
f	200	60	0.5	39.12	0.282
g	175	60	0.6	47.44	0.275
h	200	60	0.6	56.90	0.277

Table 1. The variants of quark-electron plasma.

denning and Weigel [18], based on the "HEA" and "$Bonn$" meson-exchange potentials [19–21], by taking into account two-particle correlations in the λ^{00}-approximation [22, 23] ($3.56 \cdot 10^{13}$g/cm^3 $< \rho <$ $4.81 \cdot 10^{14}$g/cm^3). These EoS and the corresponding EoS for nucleon component of layered neutron star matter are labeled by "HEA" and "$Bonn$". These are joined with the EoS of neutron star matter for lower density ranges [24]. As an example of a more stiff EoS (compared with the above mentioned HEA and $Bonn$ EoS) the "$BJ-V$" EoS [25] was used in the same density range.

Note that the conditions for the phase transition to a quark phase and thermodynamic equilibrium with the nucleon component, as it is seen from our analysis, are realized only for eleven EoS from the considered twenty four ones. Furthermore, for all the three used models of neutron matter the equilibrium and simultaneous coexistence with the quark EoS variants e, g and h having high values of ε_{min}, is impossible.

3. Superdense configurations with a strange quark core. Results and Discussion

The integral and structural parameters for models of calculated series of superdense layered stellar configurations are presented in this section, and their thorough investigation for some characteristic configurations is carried out. Among the basic parameters are the calculated stellar radius R, gravitational mass M, rest mass M_0, proper mass M_p, the mass and radius of the strange quark core M_{core} and R_{core}, respectively, relativistic moment of inertia I and gravitational redshift on the surface of the star Z_s. Also given here is the accumulated mass M_{Aen} and the radial coordinate R_{Aen}, corresponding to the threshold for evaporation of neutrons from nuclei ($\rho_{nd} = 4.3 \cdot 10^{11}$g/cm^3). In models of EoS with $\lambda < 3/2$ (in our work seven) a kink (fracture) on the $M(P_c)$ curve without a change of derivative sign appears at the beginning of formation of quark-phase core at the center of the star (the transition to a quark

phase does not cause instability). In the opposite case ($\lambda > 3/2$) at the threshold of formation of quark-phase core a descending branch on the $M(P_c)$ curve occurs; the configurations on this branch are unstable (the so-called instability of configurations with small-mass cores); thus, the local toothlike maximum (kink) arises on the $M(P_c)$ curve. Table 2 gives the basic integral parameters for the four characteristic configurations A, B, F and G obtained using the seven EoS with $\lambda < 3/2$. It also gives the parameters of the first-order phase transition – the values of transition pressure P_0 and energy densities ρ_N and ρ_Q at the transition point in the nucleon and quark phases, respectively. The EoS with phase transition are labeled as follows: the numbers refer to the nuclear EoS with 1 corresponding to HEA, 2 – to $Bonn$, 3 – to $BJ - V$; the letters refer to the corresponding quark model (see Table 1). The relativistic parameter of density jump $\lambda = \rho_Q/(\rho_N + P_0/c^2)$ is given as well; its value determines the stability ranges of layered models on the curve of the dependence of star mass M on the central pressure P_c [26, 28]. The configuration A corresponds to a point of loss of stability in the low-mass range on the $M(P_c)$ curve. These configurations have no quark core. The bulk of their mass is concentrated in "Aen" plasma (which consists of degenerated neutrons and electrons, and neutron-rich atomic nuclei). The radius of this range is of the order of $10 - 11$ km. However the whole radius of these configurations, which varies from 200 km to 250 km, is mainly determined by the so-called "Ae" - matter (matter composed of atomic nuclei and electrons), and the packing factor $\alpha = (M_0 - M)/M_0$ is within the interval $(3 \div 6) \cdot 10^{-3}$, i.e. of the same order of magnitude as for white dwarfs. Configurations B label the models of neutron stars with the central pressure corresponding to the threshold for formation of a quark core. For these models the values of the packing factor α are within $(1.8 \div 7.5) \cdot 10^{-2}$, and the gravitational redshift from the star surface varies in the interval $(3.3 \div 13) \cdot 10^{-2}$. Configurations F represent the models of layered neutron stars with the observationally inferred mass $1.44\ M_\odot$ [27]. Configurations G represent layered neutron stars with a maximal possible mass, i.e. the mass beyond which the stability loss occurs. The values of the maximal mass M_{max} are within $(1.69 \div 1.83)\ M_\odot$. For all the four calculated EoS with $\lambda > 3/2$ whose critical configurations are given in the Table 3, the transition pressure is much less than in models considered above. The toothlike kink characteristic for models with $\lambda > 3/2$ on the $M(P_c)$ curve is well seen for all these EoS, however it is located in the low-mass range for models $1a$, $2a$ and $3b$. Apart from this feature, we found that for the three EoS ($1a$, $2a$ and $3a$) a new additional local maximum is formed on the $M(P_c)$ curve after the characteristic kink.

Such models were obtained and calculated for the first time in Refs. [**?**, **?**]. The appearance of the second local maximum implies the existence of a new family of stable equilibrium stellar configurations - the neutron stars with a

	P_c MeV/fm^3	$\rho_c 10^{-14}$ g/cm^3	R_{core} km	M_{core} $M_\odot$	R_{Aen} km	m_{Aen} $M_\odot$	R km	M $M_\odot$	M_0 $M_\odot$	I $M_\odot km^2$	z_s
EoS 1b	$P_0 = 5.98 MeV/fm^3$,	$\rho_N = 3.49 \cdot 10^{14} g/cm^3$,	$\rho_Q = 4.86 \cdot 10^{14} g/cm^3$,	$\lambda = 1.35$							
A	0.74	2.05	0	0	11.35	0.076	245.01	0.0806	0.0811	9.439	$4.9 \cdot 10^{-4}$
B	5.98	4.86	0	0	9.91	0.318	12.22	0.3184	0.3273	8.776	$4.1 \cdot 10^{-2}$
F	77.53	9.07	9.751	1.209	11.34	1.441	11.73	1.4411	1.6245	74.628	$2.5 \cdot 10^{-1}$
G	321.97	22.80	9.775	1.707	10.67	1.831	10.88	1.8315	2.1431	90.304	$4.1 \cdot 10^{-1}$
EoS 2b	$P_0 = 5.67 MeV/fm^3$,	$\rho_N = 3.52 \cdot 10^{14} g/cm^3$,	$\rho_Q = 4.84 \cdot 10^{14} g/cm^3$,	$\lambda = 1.34$							
A	0.74	2.01	0	0	11.26	0.075	259.07	0.0798	0.0803	10.351	$4.5 \cdot 10^{-4}$
B	5.67	4.84	0	0	9.93	0.305	12.40	0.3048	0.3129	8.317	$3.8 \cdot 10^{-2}$
F	77.53	9.07	9.786	1.219	11.34	1.440	11.73	1.4400	1.6230	74.466	$2.5 \cdot 10^{-1}$
G	322.57	22.83	9.793	1.713	10.66	1.831	10.87	1.8311	2.1425	90.213	$4.1 \cdot 10^{-1}$
EoS 2c	$P_0 = 14.11 MeV/fm^3$,	$\rho_N = 4.13 \cdot 10^{14} g/cm^3$,	$\rho_Q = 5.26 \cdot 10^{14} g/cm^3$,	$\lambda = 1.20$							
A	0.74	2.01	0	0	11.26	0.075	259.07	0.0798	0.0803	10.351	$4.5 \cdot 10^{-4}$
B	14.11	4.13	0	0	11.13	0.686	12.22	0.6864	0.7252	28.894	$9.5 \cdot 10^{-2}$
F	67.28	8.31	8.723	0.879	11.84	1.440	12.27	1.4400	1.6119	79.270	$2.4 \cdot 10^{-1}$
G	170.52	14.07	9.611	1.438	11.58	1.820	11.85	1.8200	2.1075	103.110	$3.5 \cdot 10^{-1}$
EoS 3c	$P_0 = 6.01 MeV/fm^3$,	$\rho_N = 4.08 \cdot 10^{14} g/cm^3$,	$\rho_Q = 4.79 \cdot 10^{14} g/cm^3$,	$\lambda = 1.14$							
A	0.49	1.50	0	0	12.87	0.088	197.84	0.0931	0.0934	9.379	$6.9 \cdot 10^{-4}$
B	6.01	4.79	0	0	10.46	0.307	13.21	0.3072	0.3133	8.676	$3.6 \cdot 10^{-2}$
F	73.09	8.63	9.818	1.200	11.54	1.442	11.94	1.4419	1.6106	76.082	$2.5 \cdot 10^{-1}$
G	170.52	14.07	10.225	1.629	11.38	1.799	11.65	1.7989	2.0760	99.515	$3.5 \cdot 10^{-1}$
EoS 2d	$P_0 = 11.22 MeV/fm^3$,	$\rho_N = 3.97 \cdot 10^{14} g/cm^3$,	$\rho_Q = 5.46 \cdot 10^{14} g/cm^3$,	$\lambda = 1.31$							
A	0.74	2.01	0	0	11.26	0.080	257.43	0.0798	0.0803	10.211	$4.6 \cdot 10^{-4}$
B	11.22	3.97	0	0	10.76	0.561	12.07	0.5612	0.5875	21.040	$7.7 \cdot 10^{-2}$
F	82.86	9.57	9.004	1.044	11.39	1.440	11.78	1.4400	1.6181	73.480	$2.5 \cdot 10^{-1}$
G	335.80	23.59	9.281	1.594	10.60	1.806	10.81	1.8059	2.1029	86.368	$4.0 \cdot 10^{-1}$
EoS 3d	$P_0 = 5.29 MeV/fm^3$,	$\rho_N = 3.87 \cdot 10^{14} g/cm^3$,	$\rho_Q = 5.12 \cdot 10^{14} g/cm^3$,	$\lambda = 1.29$							
A	0.49	1.50	0	0	12.87	0.088	197.84	0.0931	0.0934	9.379	$6.9 \cdot 10^{-4}$
B	5.29	5.12	0	0	10.47	0.285	13.54	0.2852	0.2903	7.937	$3.3 \cdot 10^{-2}$
F	87.70	9.84	9.667	1.254	11.14	1.440	11.51	1.4402	1.6158	71.301	$2.6 \cdot 10^{-1}$
G	345.68	24.13	9.592	1.695	10.44	1.796	10.64	1.7960	2.0873	84.363	$4.1 \cdot 10^{-1}$
EoS 2f	$P_0 = 20.27 MeV/fm^3$,	$\rho_N = 4.48 \cdot 10^{14} g/cm^3$,	$\rho_Q = 6.10 \cdot 10^{14} g/cm^3$,	$\lambda = 1.26$							
A	0.74	2.01	0	0	11.26	0.075	259.07	0.0798	0.0803	10.351	$4.5 \cdot 10^{-4}$
B	20.27	6.10	0	0	11.75	0.925	12.57	0.9256	0.9947	46.547	$1.3 \cdot 10^{-2}$
F	76.89	9.41	7.854	0.737	11.76	1.440	12.18	1.4401	1.6101	77.138	$2.4 \cdot 10^{-1}$
G	148.15	13.46	8.708	1.155	11.47	1.687	11.77	1.6871	1.9289	90.158	$3.2 \cdot 10^{-1}$

Table 2: The basic integral and structural parameters of characteristic configurations for equations of state with $\lambda < 3/2$.

	P_c MeV/fm^3	$\rho_c 10^{-14}$ g/cm^3	R_{core} km	M_{core} $M_\odot$	R_{Aen} km	m_{Aen} $M_\odot$	R km	M $M_\odot$	M_0 $M_\odot$	I $M_\odot km^2$	Z_s
	EoS 1a	$P_0 = 0.761 MeV/fm^3$,	$\rho_N = 2.08 \cdot 10^{14} g/cm^3$,	$\rho_Q = 4.47 \cdot 10^{14} g/cm^3$,	$\lambda = 2.13$						
A	0.741	2.060	0	0	11.35	0.076	248.33	0.0806	0.0811	9.70	$4.8{\cdot}10^{-4}$
B	0.761	4.467	0	0	11.29	0.077	197.21	0.0807	00812	6.25	$6.0{\cdot}10^{-4}$
C	1.086	4.487	1.355	0.002	11.25	0.073	515.51	0.0798	0.0803	58.50	$2.3{\cdot}10^{-4}$
D	1.195	4.493	1.562	0.004	11.17	0.072	702.63	0.0799	0.0804	145.04	$1.7{\cdot}10^{-4}$
E	1.975	4.539	2.582	0.016	10.02	0.070	131.06	0.0723	0.0727	2.37	$8.1{\cdot}10^{-4}$
F	74.469	8.719	10.494	1.408	11.41	1.439	11.05	1.4392	1.6359	74.79	$2.6{\cdot}10^{-1}$
G	296.296	21.054	10.332	1.845	10.85	1.863	10.65	1.8626	2.2039	95.49	$4.2{\cdot}10^{-1}$
	EoS 2a	$P_0 = 0.758 MeV/fm^3$,	$\rho_N = 2.03 \cdot 10^{14} g/cm^3$,	$\rho_Q = 4.47 \cdot 10^{14} g/cm^3$,	$\lambda = 2.19$						
A	0.741	2.014	0	0	11.26	0.075	259.07	0.0798	0.0803	10.35	$4.5{\cdot}10^{-4}$
B	0.758	4466	0	0	11.21	0.076	207.21	0.0799	0.0807	6.65	$5.7{\cdot}10^{-4}$
C	0.939	4.478	1.012	0.003	11.25	0.074	386.02	0.0795	0.0802	26.41	$3.0{\cdot}10^{-4}$
D	1.294	4.498	1.734	0.005	10.99	0.070	1304.5	0.0820	0.0827	1062.00	$9.3{\cdot}10^{-5}$
E	1.975	4.539	2.586	0.016	9.95	0.069	133.88	0.0717	0.0724	2.38	$7.9{\cdot}10^{-4}$
F	74.568	8.724	10.496	1.409	11.05	1.440	11.41	1.4400	1.6369	74.85	$2.6{\cdot}10^{-1}$
G	320.988	22.410	10.264	1.847	10.57	1.863	10.77	1.8635	2.2052	94.12	$4.3{\cdot}10^{-1}$
	EoS 3a	$P_0 = 0.199 MeV/fm^3$,	$\rho_N = 0.86 \cdot 10^{14} g/cm^3$,	$\rho_Q = 4.43 \cdot 10^{14} g/cm^3$,	$\lambda = 5.11$						
A	0.035	0.277	0	0	18.17	0.052	893.6	0.6101	0.6157	$2.4{\cdot}10^{4}$	$1.0{\cdot}10^{-3}$
B	0.199	4.433	0	0	14.58	0.072	2214.6	0.6386	06444	$2.4{\cdot}10^{4}$	$4.3{\cdot}10^{-4}$
C	0.395	4.445	1.07	0.001	14.90	0.066	1708.3	0.6360	0.6418	$1.2{\cdot}10^{5}$	$5.5{\cdot}10^{-4}$
D	2.123	4.547	3.25	0.032	8.29	0.046	2696.5	0.8200	0.8277	$6.3{\cdot}10^{4}$	$4.5{\cdot}10^{-4}$
E	2.395	4.563	3.46	0.039	7.75	0.051	361.7	0.0534	0.0535	9.20	$2.2{\cdot}10^{-4}$
F	74.568	8.724	10.57	1.431	10.93	1.439	11.29	1.4390	1.6356	74.71	$2.7{\cdot}10^{-1}$
G	316.049	22.139	10.32	1.900	10.53	1.863	10.72	1.863	2.2047	94.35	$4.3{\cdot}10^{-1}$
	EoS 3b	$P_0 = 0.796 MeV/fm^3$,	$\rho_N = 1.73 \cdot 10^{14} g/cm^3$,	$\rho_Q = 4.54 \cdot 10^{14} g/cm^3$,	$\lambda = 2.61$						
A	0.494	1.505	0	0	12.87	0.088	197.84	0.0931	0.0934	9.38	$6.9{\cdot}10^{-4}$
B	0.796	4.543	0	0	11.95	0.102	48.49	0.1042	0.1047	3.17	$3.2{\cdot}10^{-3}$
C	2.222	4.631	2.74	0.020	10.75	0.087	53.78	0.0885	0.0887	1.94	$2.4{\cdot}10^{-3}$
F	79.506	9.180	10.39	1.408	11.00	1.439	11.36	1.4393	1.6209	73.28	$2.6{\cdot}10^{-1}$
G	325.926	23.019	10.11	1.809	10.47	1.826	10.67	1.8262	2.1348	89.24	$4.2{\cdot}10^{-1}$

Table 3: The basic integral and structural parameters of characteristic configurations for equations of state with $\lambda > 3/2$.

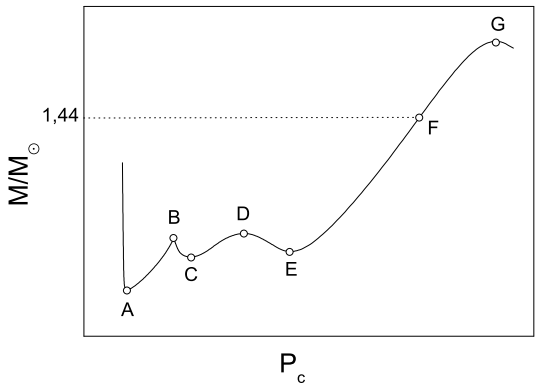

Figure 1. Schematic arrangement of characteristic configurations; their parameters are tabulated in Tables 2 and 3.

strange quark core, which may have interesting distinctive features. In particular, the configurations of this new additional stable branch have radii in excess of a thousand kilometer. In Table 3 besides the four mentioned critical configurations as above, for EoS $1a$, $2a$ and $3a$ the parameters of configurations C, D and E describing this new local maximum, and for EoS $3b$– configuration C describing the minimum after the kink attributable to the formation of quark phase, are given. The branch AB represents stable neutron stars without a quark core, and CD– stable configurations having small quark core. While in the case of EoS $1a$ and $2a$ the toothlike kink and the new local maximum are located in the low-mass range ($M \approx 0.08 M_\odot$), for the model $3a$ both the branch AB and the following additional stable branch CD move to the mass range of $\approx 0.6 M_\odot$. As it is seen from Fig. $2c$, in the density range $3.5 \cdot 10^{13}$ g/cm^3 $\leq \rho_c \leq 8.6 \cdot 10^{13}$ g/cm^3 the derivative $dM/d\rho_c$ is positive and corresponds to the stable white dwarfs of medium masses with a small central region (core), composed of neutron-rich atomic nuclei and degenerated neutrons and electrons. The critical (limiting) configuration of this stable branch (before the transition to the quark phase) has the following parameters: $M_{max} = 0.638 M_\odot$, $R_{max} = 2195$ km, the packing factor $\alpha = 9 \cdot 10^{-3}$, $M_{Aen} = 0.072 M_\odot$, $R_{Aen} = 14.6$ km.

In the case of EoS $3a$, unlike the other EoS with $\lambda > 3/2$, the values of M_{Aen}/M and R_{Aen}/R for configuration B are equal to 0.11 and $6.6 \cdot 10^{-3}$, respectively, i.e. these models are mainly composed of usual white dwarf matter. On the both branches AB and CD the packing factor α has the values typical for massive white dwarfs. While for EoS $1a$ $M_B > M_D$, in the case of EoS $2a$ and $3a$ the opposite is true, $M_D > M_B$. This fact makes it possible for the stars described by the latter two EoS a transition from configuration B to more dense configurations through two restructurings when there is an accre-

tion of matter on the star: first to a configuration of the branch CD, and then – to the main ascending branch of stable neutron stars with a strange quark core. As a result, there will be two successive energy releases [**?**, **?**].

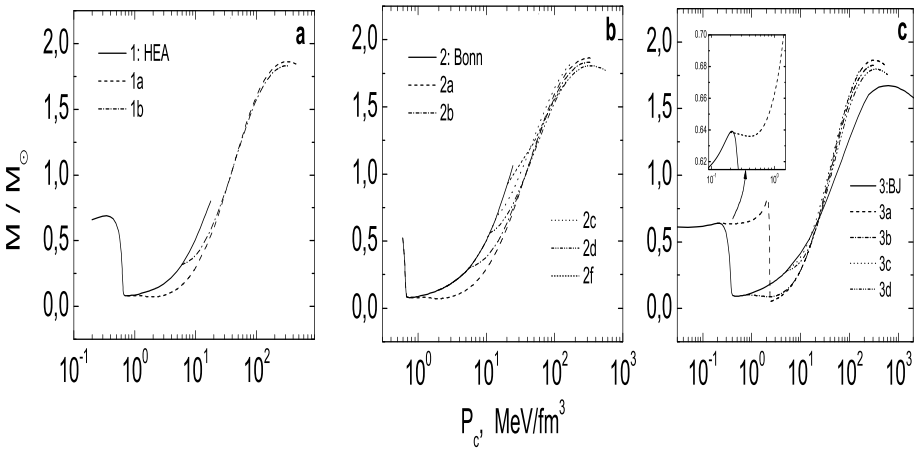

Figure 2. The dependences of gravitational mass M on central pressure P_c for the sets of EoS with variants $HEA(a)$, $Bonn(b)$ and $BJ-V(c)$. Solid lines correspond to the models of neutron stars without a quark core (the variant of nucleon component is indicated). On an enlarged scale the phase transition area is shown for EoS $3a$.

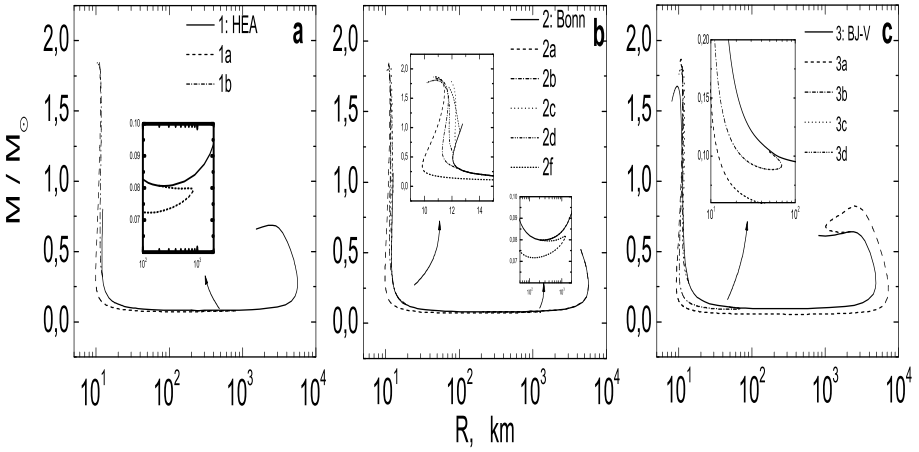

Figure 3. Mass M versus radius R. On an enlarged scale the new additional local mass maximum is shown for neutron stars with a strange quark core. In the upper left corner of Fig. 3b, the phase transition area is shown for the whole set of EoS.

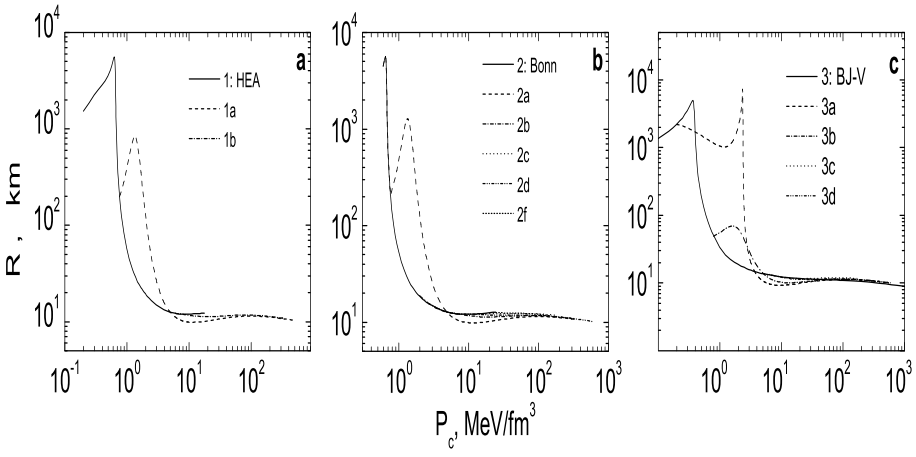

Figure 4. The dependences of the radius R on central pressure P_c (the EoS are denoted as in Fig.2,3).

The dependences of the gravitational mass M on the central pressure P_c, the mass M on the radius R, and the radius R on the central pressure P_c for the sets of EoS with nucleon variants $HEA\,(a)$, $Bonn\,(b)$ and $BJ-V\,(c)$ are presented in Figs. 2, 3, and 4, respectively.

4. Summary

First-order phase transition from a nucleonic matter to the strange quark state with a transition parameter $\lambda > 3/2$ that occurs in superdense nuclear matter generally gives rise to a toothlike kink on the stable branch of the dependence of stellar mass on central pressure. Based on the extensive set of calculated realistic equations of state of superdense matter, we revealed a new stable branch of superdense configurations. The new branch emerges for some of our models with the transition parameter $\lambda > 3/2$ and a small quark core ($M_{core} \sim 0.004 \div 0.03 M_\odot$) on the $M(P_c)$ curve, with $M_{max} \sim 0.08 M_\odot$ and $M_{max} \sim 0.82 M_\odot$ for different equations of state. Stable equilibrium layered neutron stars, located in these additional ranges of stability, are characterized also by unusually large values of the stellar radius (from $R \sim 1300$ km to ~ 2700 km in different models). It should be noted that for such equations of state (if $M_D > M_B$), accretion onto a neutron star will lead to two successive jumplike transitions to a quark-core neutron star; as a result, there will be two successive energy releases.

Acknowledgments

This work was supported by the Armenian National Science and Education Foundation (ANSEF Grant No. PS 140) and the Ministry of Education and Science of the Republic of Armenia within the framework of the topic No. 0842.

References

[1] E. Witten, Phys. Rev. D. 30, 272 (1984).

[2] P. Haensel, J. L. Zdunik, R. Schaeffer,Astron. Astrophys. 160, 121 (1986).

[3] Yu. L. Vartanyan, A. R. Arutyunyan, A. K. Grigoryan, Astronomy Letters 21, 122 (1995).

[4] P. A. Carinhas, Astrophys. J. 412, 213 (1993).

[5] G. B. Alaverdian, A. R. Harutyunian, Yu. L. Vartanian, A. K. Grigorian, Rep. Nat. Acad. Sci. of Armenia, Physics 95, 98 (1995).

[6] G. B. Alaverdyan, A. R. Harutyunyan, Yu. L. Vartanyan, Astrophysics 44, 265 (2001).

[7] G. B. Alaverdyan, A. R. Harutyunyan, Yu. L. Vartanyan, Spacetime and Substance 2, No.3(8), 129 (2001).

[8] G. B. Alaverdyan, A. R. Arutyunyan, Yu. L. Vartanyan, Astronomy Letters 28, 24 (2002).

[9] A. R. Harutyunyan, Astrophysics 45, 248 (2002).

[10] H. Heiselberg, C. J. Pethick, E. F. Staubo, Phys. Rev. Lett. 70, 1355 (1993).

[11] C. P. Lorenz, D. G. Ravenhall, C. J. Pethick, Phys. Rev. Lett. 70, 379 (1993).

[12] N. K. Glendenning, astro-ph/9706236 (1997).

[13] H. Heiselberg, M. Hjorth-Jensen, Phys.Rept.328:237-327 (1999).

[14] eds. D. Blaschke, N. K. Glendenning, A. Sedrakian, Physics of Neutron Star Interiors. Berlin (2001).

[15] N. K. Glendenning, Phys. Rev. D. 46, 1274 (1992).

[16] D. N. Voskresensky, M. Yasuhira, T. Tatsumi, Nucl. Phys. A. 723, 291 (2003).

[17] A. Chodos, R. L. Jaffe, K. Johnson, C. B. Thorn, V. F. Weisskopf, Phys. Rev. D. 9, 3471 (1974).

[18] F. Weber, N. K. Glendenning, M. K. Weigel, Astrophys. J. 373, 579 (1991).

[19] R. Machleidt, K. Holinde, Ch. Elster, Phys. Rep. 149, 1 (1987).

[20] K. Holinde, K. Erkelenz, R. Alzetta, Nucl. Phys. A. 194, 161 (1972).

[21] K. Holinde, K. Erkelenz, R. Alzetta, Nucl. Phys. A. 198, 598 (1972).

[22] P. Poschenrieder, M. K. Weigel, Phys. Lett. B. 200, 231 (1988).

[23] P. Poschenrieder, M. K. Weigel, Phys. Rev. C. 38, 471 (1988).

[24] G. S. Bisnovatyi-Kogan, Physical Problems of the Theory of Stellar Evolution. Moscow (1989).

[25] R. C. Malone, M. B. Johnson, H. A. Bethe, Astrophys. J. 199, 741 (1975).

[26] Z. F. Seidov, Sov. Astron.Zh. 15, 347 (1971).

[27] J. H. Taylor, J. M. Weisberg, Astrophys.J. 345, 434 (1989).

[28] P. Haensel, M. Proszynski, Astrophys.J. 258, 306 (1982).